ACS APPLIED MATERIALS & INTERFACES

Research Article

www.acsami.org

Iron Oxide Nanoparticles Grafted with Sulfonated Copolymers are Stable in Concentrated Brine at Elevated Temperatures and Weakly Adsorb on Silica

Hitesh G. Bagaria,[†,‡] Zheng Xue,[†,‡] Bethany M. Neilson,[§] Andrew J. Worthen,[†] Ki Youl Yoon,[†] Susheela Nayak,[†] Victoria Cheng,[†] Jae Ho Lee,[†] Christopher W. Bielawski,[§] and Keith P. Johnston*[,†]

[†]Department of Chemical Engineering and [§]Department of Chemistry and Biochemistry, University of Texas at Austin, Austin, Texas 78712, United States

Supporting Information

ABSTRACT: Magnetic nanoparticles that can be transported in subsurface reservoirs at high salinities and temperatures are expected to have a major impact on enhanced oil recovery, carbon dioxide sequestration, and electromagnetic imaging. Herein we report a rare example of steric stabilization of iron oxide (IO) nanoparticles (NPs) grafted with poly(2-acrylamido-2-methylpropanesulfonate-*co*-acrylic acid) (poly(AMPS-*co*-AA)) that not only display colloidal stability in standard American Petroleum Institute (API) brine (8% NaCl + 2% $CaCl_2$ by weight) at 90 °C for 1 month but also resist undesirable adsorption on silica surfaces (0.4% monolayer NPs). Because the AMPS groups interacted weakly with Ca^{2+}, they were sufficiently well solvated to provide steric stabilization. The PAA groups, in contrast, enabled covalent grafting of the poly(AMPS-*co*-AA) chains to amine-functionalized IO NPs via formation of amide bonds and prevented polymer desorption even after a 40 000-fold dilution. The aforementioned methodology may be readily adapted to stabilize a variety of other functional inorganic and organic NPs at high salinities and temperatures.

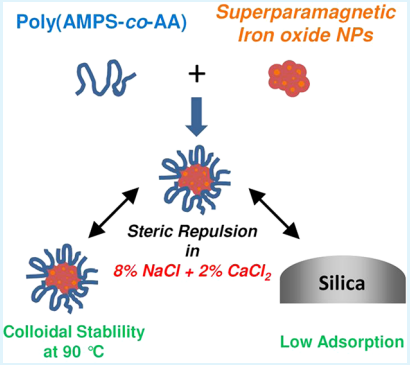

KEYWORDS: *poly(2-acrylamido-2-methylpropanesulfonate-co-acrylic acid), superparamagnetic nanoparticles, steric stabilization, high salinity, multipoint grafting, magnetite nanoparticles, electromagnetic imaging*

INTRODUCTION

Interest in nanotechnology for subsurface applications, including oil and gas recovery, reservoir imaging,[1,2] CO_2 sequestration,[3−5] and environmental remediation,[6−8] has grown markedly over the past few years. In particular, superparamagnetic iron oxide nanoparticles (NPs) that have been utilized in biomedical MRI imaging[9,10] are now being explored for subsurface applications including magnetomotive acoustic imaging[11,12] and cross-well electromagnetic tomography.[13,14] These developments offer the potential to monitor reservoir fluid movement and composition between oil wells separated by hundreds of meters if NPs can be transported successfully through the reservoir. Unfortunately, the high salinities (>1 M) and often elevated temperatures (≤150 °C) found in subsurface reservoirs cause NP aggregation as well as excessive nanoparticle adsorption on mineral surfaces.[6,8,11,12,15] NP stabilizers may be used to attempt to overcome this drawback, but with limited success. At high ionic strength, extensive charge screening in very thin double layers weakens electrostatic repulsion between particles.[11] While ionic[6,16−18] and zwitterionic[19] polymers have been shown to provide sufficient steric and electrosteric stabilization in aqueous NaCl up to 5 M,[16,17] at ambient temperature, colloidal stabilization is unknown at elevated temperatures (50−150 °C), especially when concentrated divalent ions are present.

Of the aforementioned materials, the polymeric stabilizers have the potential to prevent NP flocculation if the pure polymer in the same solvent does not undergo phase separation.[20,21] Weak polyelectrolytes, such as poly(acrylic acid) (PAA) remain soluble in 1 M NaCl at 90 °C,[22] but precipitate in the presence of Ca^{2+} at ambient temperature due to specific-ion complexation and hydration, as shown by NMR spectroscopy and calorimetry.[23,24] In contrast, highly acidic sulfonated polymers exhibit low Ca^{2+} binding affinities and remain soluble even at high temperatures, especially those containing high levels of styrenesulfonate (PSS) or 2-acrylamido-2-methylpropanesulfonate (PAMPS).[25−27] Moreover, when adsorbed on NP surfaces, soluble polyelectrolyte chains do not collapse and provide steric and electrosteric stabilization.[6,17,20,28] For example, PAA or polymethacrylic acid (PMAA) stabilize latexes[17,29] and IO NPs in aqueous solutions of Na^+ or K^+ (up to 3.5 M) at room temperature, although the introduction of low quantities Ca^{2+} and Mg^{2+} ions (5 mM)

Received: January 29, 2013
Accepted: March 25, 2013
Published: March 25, 2013

 © 2013 American Chemical Society dx.doi.org/10.1021/am4003974 | *ACS Appl. Mater. Interfaces* 2013, 5, 3329−3339

induce flocculation.[30] IO NPs with adsorbed random copolymers of PAA, PSS, and poly(vinylsulfonic acid) (PVS) were stable in 5 M NaCl at room temperature.[16] Furthermore, PSS-based copolymers stabilized NP dispersions in relatively dilute solutions of 0.1 M Mg^{2+}[31] or Ca^{2+}[6] at room temperature. The same anionic polymers that provide repulsion between NPs also have the potential to minimize adsorption on negatively charged bulk surfaces (e.g., silica). However, studies of transport of polymer-stabilized NPs in porous media,[6,8] as well as NP adsorption isotherms[7,32,33] have not examined high salinities, particularly with divalent ions. Here, charge screening weakens electrostatic repulsion between the particles and the substrate, and furthermore, divalent cations may bridge anionic nanoparticles to negatively charged silica. Given these extreme and unusual conditions, it is very unclear as to whether low nanoparticle adsorption levels would be possible.

A further problem in porous media is that the large volumes of water and mineral surface areas provide a strong thermodynamic driving force for desorption of adsorbed polymers from NP surfaces. PAA-based polymers adsorbed on iron oxide by only charge-transfer complexes,[16,18,34] are readily susceptible to desorption.[35] Alternatively, for more permanent attachment, predesigned polymers with the desired composition and molecular weight may be covalently attached to NP surface by the "grafting to" technique.[19,36−41] A large number of anchor groups would be desirable for multipoint covalent grafting to enhance stability, especially in harsh environments.[42,43] The need therefore remains to design copolymers which may facilitate multipoint grafting without compromising the solubility in concentrated brines at elevated temperatures.

Herein we report the design and synthesis of iron oxide (IO) NPs that have been covalently grafted with sulfonated copolymers. These materials were discovered to form stable dispersions in highly concentrated brine (API brine; 8 wt % NaCl + 2 wt % $CaCl_2$,1.8 M total ionic strength) that includes the presence of large quantities of $CaCl_2$ (0.18 M) at 90 °C, while exhibiting minimal adsorption on silica microparticles. The aforementioned copolymer, poly(2-methyl-2-acrylamido-propanesulfonate-*co*-acrylic acid) (poly(AMPS-*co*-AA) 3:1), was designed to contain a high proportion of AMPS stabilizer groups to provide a low binding affinity for calcium ions as well as a proper fraction of AA anchor groups to enable covalent attachment. Indeed, the copolymer was covalently grafted to amine-functionalized IO NPs, which prevented desorption from the IO surface even after a 40,000-fold serial dilution. The hydrodynamic diameter of the pure polymer, as measured by DLS, underwent little contraction at high salinity and elevated temperatures, reflecting weak interactions with Ca^{2+}. Consequently, favorable solvation of the extended poly(AMPS-*co*-AA) brushes on the IO surface enabled steric stabilization between NPs, and between NPs and the silica surfaces, resulting in extremely low nanoparticle adsorption (0.4% monolayer).

EXPERIMENTAL SECTION

Materials. Iron(II) chloride tetrahydrate, iron(III) chloride hexahydrate, citric acid monohydrate, 30% ammonium hydroxide, 3-aminopropyl triethoxy silane (APTES), glacial acetic acid, calcium chloride dihydrate, sodium chloride, hydrochloric acid, sodium hydroxide, 1-ethyl-3-(3-dimethylaminopropyl)carbodiimide (EDC), acrylic acid, potassium persulfate, sodium metabisulfite, and poly(acrylic acid) sodium salt (5 kDa) were obtained from commercial sources and used as received. The monomer 2-amino-2-methylpropanesulfonate (AMPS) was a gift from Lubrizol corporation and used as received. Uniformly sized (see Figure S1 in the Supporting Information) colloidal silica microspheres (8 μm, product number SIOP800−01−1KG) with a surface area of 0.58 m^2/g (as measured by BET) were purchased from Fiber Optic Center Inc., New Bedford, MA, USA, and were washed at least five times with deionized (DI) water, obtained from a Barnstead Nanopure system, before use to remove smaller particles.

Synthesis of Poly(2-acrylamido-3-methylpropanesulfonate-co-acrylic acid) (poly(AMPS-co-AA) 3:1). A three-necked round-bottom flask equipped with a magnetic stir bar, a nitrogen inlet and a reflux condenser was charged with 30.9 g (0.135 mol) of AMPS monomer, 4.86 g (0.018 mol) of potassium persulfate and 3.42 g (0.018 mol) of sodium metabisulfite under an atmosphere of nitrogen. The flask was sealed with a rubber septum and 180 mL of deionized water that was previously degassed by bubbling with nitrogen for 30 min was added via a cannula to the reaction flask. With stirring, 3.0 mL (0.044 mol) of acrylic acid was added to the reaction flask via a nitrogen-purged syringe. The total monomer concentration at the start of the reaction was 1.0 M. The flask was placed in an oil bath thermostatted at 80 °C and stirred at that temperature under nitrogen for 16 h. The reaction mixture was then cooled to room temperature and the water was removed under reduced pressure. The resulting white solid was then dried under reduced pressure until a constant mass (43.14 g) was reached. ^{1}H NMR (400 MHz, D_2O): δ 0.96 (m, br, 10H, backbone CH_2 of AMPS and AA, and CH_3 of AMPS), 1.60 (br, 2H, backbone CH of AMPS and AA), 2.83 (br, s, 2H, CH_2SO_3Na of AMPS). ^{13}C NMR (100 MHz, D_2O): δ 26.2 (CH_3 of AMPS), 34.4 (CH_2 of backbone), 42.0 (CH of backbone), 52.1 (CH_2SO_3Na of AMPS), 57.5 ($CCH_2(CH_3)_2NH$ of AMPS), 175.4 (CONH of AMPS), 178.4 (COOH of AA). IR (ATR): ν 2943.1, 1719.9, 1654.7, 1555.6, 1455.9, 1173.7, 1040.9, 884.4, 850.1.

Synthesis of Iron Oxide Nanoparticles (IO NPs). IO NPs were prepared by the coprecipitation of Fe(II) and Fe(III) chlorides in an alkaline solution.[44,45] Briefly, a mixture of 2.15 g of $FeCl_2{\cdot}4H_2O$ and 5.87 g of $FeCl_3{\cdot}6H_2O$ (1:2 mol ratio) and 0.125 g of citric acid were dissolved in 100 mL of DI water. The solution was heated to 90 °C with magnetic stirring followed by injection of 25 mL of 30 wt % aqueous NH_4OH solution to nucleate the IO NPs. The NP growth was continued for 2 h at 90 °C. The mixture was then cooled to room temperature and centrifuged to recover 2.5 g of IO NPs that was dispersed in 50 mL of DI water with a Branson probe sonication microtip.

Amine-Functionalization of IO NPs. Hydrolysis and condensation of APTES was conducted by mixing 12.5 mL of APTES in 125 g of a 5 wt % acetic acid solution. After 1 h of acid hydrolysis, which has been shown to form dimers and higher oligomers of APTES,[46−48] the pH was adjusted to pH 8 using 1 N NaOH solution. The reaction mixture was further diluted with DI water followed by the addition of 50 mL of IO NP solution (2.5 g of IO) to reach a total volume of 500 mL and a final IO concentration of 0.5% w/v. The mixture was placed in a water bath at 65 °C and magnetically stirred for 24 h. The mixture was removed from the water bath and cooled to room temperature, then the NPs were separated with a strong magnet, the supernatant was discarded and the NPs were washed twice with 200 mL of DI water. Finally, the washed NPs were dispersed in 50 mL of DI water, the pH was adjusted to pH 6 with 1 N HCl, and the NPs were probe sonicated for 30 min then centrifuged at 4000 rpm for 10 min to remove large clusters. The amine-functionalized IOs (APTES IO) in the supernatant were retained for grafting poly(AMPS-*co*-AA) polymer. The typical yield at the end of APTES functionalization was 60−70% IO.

Grafting of Poly(AMPS-*co*-AA) to APTES IO. Poly(AMPS-*co*-AA) was dissolved in 1 N NaOH to pH 6, followed by addition of 20 wt % NaCl solution, DI water and APTES IO stock solution under vigorous magnetic stirring to reach a final concentration of 1% IO, 5% polymer, and 3% NaCl. The pH was again adjusted to pH 6, and after 5−10 min EDC (equimolar to PAA) was added to facilitate amide bond formation. The reaction was continued overnight at room

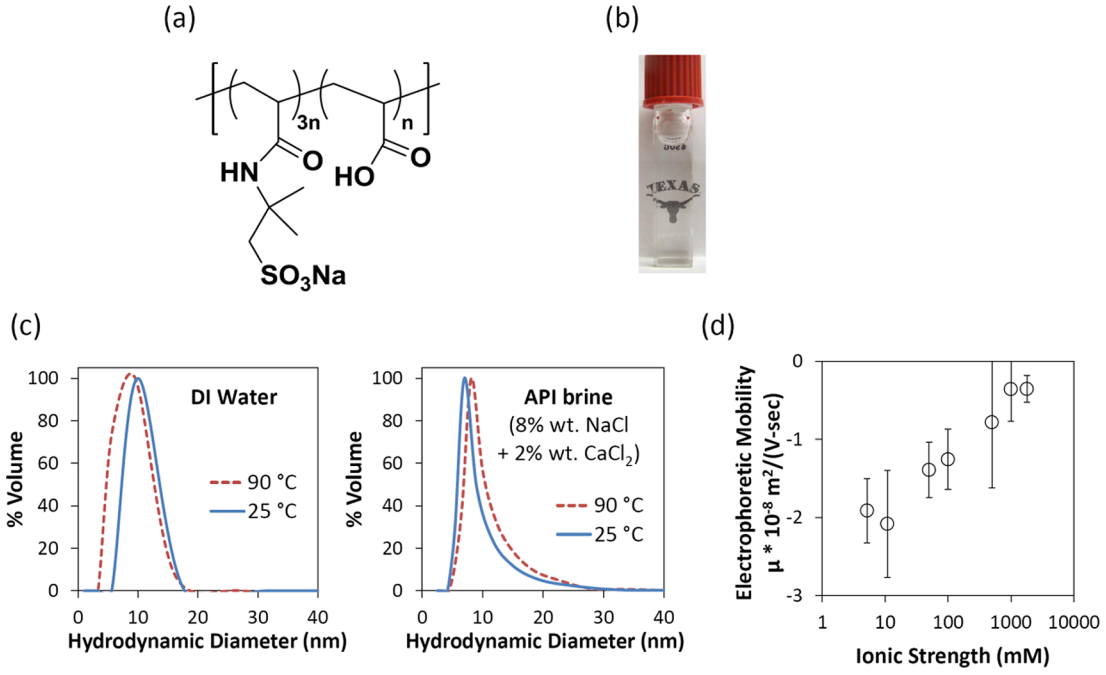

Figure 1. (a) Chemical structure of poly(2-acrylamido-2-methylpropanesulfonate-*co*-acrylic acid) (poly(AMPS-*co*-AA) 3:1); (b) poly(AMPS-*co*-AA) (3:1) remained soluble in 8 wt % NaCl + 2% $CaCl_2$ (API brine) at 90 °C as confirmed by visually clear solution; (c) volume weighted hydrodynamic diameter (D_H) of poly(AMPS-*co*-AA) (3:1) was maintained at ∼10 nm in DI water and API brine at 25 and 90 °C. (d) Electrophoretic mobility of poly(AMPS-*co*-AA) (3:1) in a series of combined Na^+ and Ca^{2+} solutions at pH 8 and fixed Na^+/Ca^{2+} mole ratio = 7.6 (same as API brine).

temperature under constant stirring. The polymer-coated iron oxide NPs were separated by centrifugation and washed with DI water twice to remove excess polymer and NaCl. The NPs were finally dispersed in DI water at ∼2% w/v IO. The typical IO yield after this procedure was 70−90% IO. Electrostatically attached poly(AMPS-*co*-AA) IO NPs were prepared for the polymer desorption test by a similar procedure, except that EDC was not added.

Adsorption of Polymer-Coated IO NPs on Silica. In a glass vial, 2 mL of aqueous dispersion of IO NPs was added to 1 g of silica. The initial concentration of IO ranged from 0.05% to 1% w/v. The glass vials were sealed and shaken overnight on a LW Scientific Model 2100A Lab Rotator at 200 rpm at room temperature, after which the mixture was left undisturbed to allow the silica adsorbent to gravimetrically sediment. The concentration of the IO NPs in the supernatant was determined by measuring the UV−vis absorbance at 575 nm after dilution of the samples, where necessary, such that the absorbance was below 2. The specific adsorption and monolayer coverage of IO nanoclusters to silica microspheres was calculated on the basis of the difference in the supernatant concentrations and volumes before and after adsorption.

Polymer Desorption Test. The poly(AMPS-*co*-AA) grafted IO NPs were diluted 200-fold to 0.01% w/v IO in 1 M NaCl solution and left undisturbed to equilibrate for 24 h to allow desorption of noncovalently attached polymer. The NPs were centrifuged at 15,000 g and dispersed in DI water after discarding the supernatant. The dilution and equilibration steps were repeated, which amounted to a 40,000-fold dilution of the initial IO solution, followed by NP separation by centrifugation and redispersion of the IO NPs in DI water by probe sonication. The final IO sample was tested for stability in API brine (8 wt % NaCl + 2 wt % $CaCl_2$) at 90 °C. As a control, a sample with electrostatically attached poly(AMPS-*co*-AA) on IO NPs (prepared without EDC) was subjected to an analogous dilution test followed by assessment of colloidal stability in API brine at 90 °C.

Characterization of Iron Oxide Nanoparticles. Dynamic light scattering (DLS) analysis was performed to measure the hydrodynamic diameter of the poly(AMPS-*co*-AA) polymer and the grafted IO NPs in DI water and API brine using a Brookhaven ZetaPlus instrument at 90° scattering angle. The built-in temperature controller was used for measurements at 25 and 90 °C. The collected autocorrelation functions were fitted with the CONTIN algorithm. All measurements were made over a period of 3 min and at least three measurements were performed on each sample. The measurements were conducted at 0.2 wt % poly(AMPS-*co*-AA) and 0.005 wt % IO NPs solution, which gave a measured count rate of approximately 35 and 500 kcps, respectively. Electrophoretic mobility of poly(AMPS-*co*-AA) polymer and grafted IO NPs was measured with a Brookhaven ZetaPALS instrument at a 15° scattering angle at room temperature. Mobility of iron oxide NPs was collected in 10 mM KCl (Debye length κ^{-1} = 3 nm). A set of 10 measurements with 30 cycles for each run were averaged. Electrophoretic mobility measurements at higher salinity were collected at 3 V and 20 Hz frequency to overcome polarization issues. Thermogravimetric analysis (TGA) was used to measure the organic content of the IO NPs after APTES functionalization and poly(AMPS-*co*-AA) grafting. All measurements were conducted using a Mettler-Toledo TGA/SDTA851e instrument under air at a heating rate of 5 °C/min from 25 to 800 °C. The percentage loss of weight was reported as the mass fraction of organic coating on the iron oxide. Transmission electron microscopy (TEM) was performed on a FEI TECNAI G2 F20 X-TWIN TEM. High-resolution images were collected with a JEOL 2010F TEM instrument. A dilute aqueous dispersion of the IO NP-clusters was deposited onto a 200 mesh carbon-coated copper TEM grid for imaging. Flame atomic absorption spectrometry (FAAS) was used to measure the concentration of iron oxide NP dispersions. All measurements were performed using a GBC 908AA flame atomic absorption spectrometer (GBC Scientific Equipment Pty Ltd.) at 242.8 nm with an air-acetylene flame. Superconducting quantum interference device (SQUID) was used to measure the magnetization curves of powders of IO NPs before and after polymer coating with a Quantum Design MPMS SQUID magnetometer. M-H loops were collected at 300 K. Liquid magnetic susceptibility was measured with a Bartington susceptometer operated at a frequency of 696 Hz.

RESULTS AND DISCUSSION

Poly(AMPS-*co*-AA) Phase Behavior, Hydrodynamic Diameter, and Electrophoretic Mobility in Brine. The random copolymer of 2-acrylamido-2-methylpropanesulfonate

(AMPS) and acrylic acid (AA) with a monomer ratio of AMPS:AA = 3:1 (poly(AMPS-*co*-AA); Figure 1a) was synthesized by aqueous free radical polymerization, and its composition was confirmed to match the monomer feed ratio by ^{1}H NMR spectroscopy (see Figure S2 in the Supporting Information). The molecular weight (MW) of the synthesized poly(AMPS-*co*-AA) was estimated by correlating the hydrodynamic diameter (D_H) to the degree of polymerization (DOP) of anionic copolymers of known MWs at pH 8 in 1 M NaCl (see Figure S3 in the Supporting Information). A similar correlation between D_H and DOP for poly(acrylic acid-*co*-styrenesulfonic acid-*co*-vinylsulfonic acid) was previously validated by static light scattering measurements.[16] The D_H of 10 nm for the poly(AMPS-*co*-AA) (3:1) translated to a DOP of approximately 1000 (750 AMPS:250 AA groups) and a MW of approximately 200 kDa. A 2 mg/mL solution of poly(AMPS-*co*-AA) remained visually clear after 24 h at 90 °C in standard "American Petroleum Institute" (API) brine composed of 8 wt % NaCl + 2 wt % $CaCl_2$ (ionic strength of 1.8 M, Figure 1b). The observed lack of phase separation under high salinity and elevated temperature has rarely been reported.[25] The polymer conformation was investigated by dynamic light scattering (DLS) to determine the hydrodynamic diameter in DI water and API brine at both 25 and 90 °C (Figure 1c). In each case, a D_H of approximately 10 nm was observed, which indicated that poly(AMPS-*co*-AA) chains did not undergo significant aggregation or collapse. In both DI water and API brine, minimal changes in D_H were observed when the temperature was increased from 25 to 90 °C.

The electrophoretic mobility (μ) of poly(AMPS-*co*-AA) was determined in a series of saline solutions with a fixed Na^+/Ca^{2+} mole ratio =7.6 (same as API brine) up to 1.8 M ionic strength at pH 8 (Figure 1d). At an ionic strength of 10 mM, a μ of -2×10^{-8} m^2/(V sec) was measured, which indicated that the poly(AMPS-*co*-AA) chains were highly charged, and that the sulfonic acid (pK_a = 1) and acrylic acid (pK_a = 4.5) groups were largely deprotonated. The magnitude of μ decreased with increasing ionic strength to a value of -0.4×10^{-8} m^2/(V s) at 1.8 M ionic strength (API brine) because of the screening of the charges by the counterions with very thin double layers at the extremely high ionic strength. However, the maintenance of a significant negative charge even at such high concentrations of both Na^+ (1.4 M) and Ca^{2+} (0.18 M) suggested to us that the Ca^{2+} ions do not fully neutralize all of the anionic sites on the poly(AMPS-*co*-AA). In contrast, the magnitude of the electrophoretic mobility for other less hydrophilic sulfonated polymers, including PSS, was reported to decrease much more rapidly even at low divalent ion concentrations of 7 mM Mg^{2+}[49,50] because of strong ion binding[51,52] and weaker hydration.

The observed effects of cations on the conformation, phase behavior and electrophoretic mobility of poly(AMPS-*co*-AA) were consistent with the previously reported behavior of the respective homopolymers in the presence of salts. PAA is a weak polyelectrolyte (pK_a = 4.5) and consequently the carboxylate anion interacts strongly with divalent counterions such as Ca^{2+} at pH ≥7,[53] which is the main reason PAA is often chosen as an anchor group for metal oxide NPs.[16,34,54] In accord with the favorable entropy for binding of Ca^{2+},[55] increased precipitation of PAA with Ca^{2+} has been observed with rising temperature.[24] Unfortunately, increasingly elevated concentration (≥1.0 mM) of Ca^{2+} leads to collapse of the PAA chains, as evidenced by significant decreases in the radius of gyration (R_g) and D_H,[24] and ultimately results in polymer precipitation.[23] In contrast to polycarboxylates, PAMPS is a much more acidic polyelectrolyte (pK_a = 1) and thus interacts more weakly with divalent cations.[25] ^{23}Na NMR spectroscopy revealed that the coupling constant for Na-PAMPS was maintained with added Ca^{2+} even at a Ca^{2+}/PAMPS molar ratio of 1.4 (0.4 mM monomer and 0.6 mM Ca^{2+}), suggesting relatively weak binding to Ca^{2+}.[27] In addition to the high acidity of the PAMPS sulfonate group, the hydrophilic amide group (Figure 1a) favors hydration, to further weaken Ca^{2+} binding.[55]

Even for polyelectrolytes like PAMPS that display weak specific ion complexation, the ionic strength has a large effect on the polymer conformation. At low salinities, the counterions in the polyelectrolyte chains produce osmotic swelling;[56−58] at very high salinities (≥1 M), however, the osmotic driving force decreases and the charges on the polyelectrolyte chain are highly screened by the presence of free ions in solution.[57,59] These two factors cause the chains to contract to the size of an uncharged polymer, as was reported for PSS[51,60] and PAA[24] in solutions of varying Ca^{2+} content. Interestingly, poly(AMPS-*co*-AA) appeared to be relatively resistant to this phenomenon, as evidenced by the slight contraction observed only in narrowing of the D_H distribution when changing from DI water to API brine (0.18 M Ca^{2+} and 1.4 M Na^+) (Figure 1c). While it is possible that the presence of Na^+ may dilute the effect of stronger interactions of poly(AMPS-*co*-AA) with Ca^{2+},[23] the observed D_H profile of poly(AMPS-*co*-AA) in pure Ca^{2+} solutions (0.18 and 0.45 M Ca^{2+}; see Figure S4 in the Supporting Information) also showed minimal contraction compared to DI water, and was nearly identical to that observed in API brine. The hydrated PAMPS groups in the copolymer chain do not bind specifically to Ca^{2+}, and furthermore mask the much more favorable Ca^{2+}-binding of the PAA groups, thereby preventing significant chain collapse. The statistical distribution of the monomer units throughout the polymer backbone places stabilizing AMPS groups adjacent to AA groups, which promotes hydration of AA and weakens Ca^{2+} binding relative to a PAA homopolymer.[24]

Subsequent efforts were directed toward examining the effect of temperature on the conformation of poly(AMPS-*co*-AA) by measuring the hydrodynamic diameter at 90 °C (Figure 1c). Remarkably, the poly(AMPS-*co*-AA) chains were observed to undergo minor contraction at high salinities (1.4 M Na^+ and 0.18 M Ca^{2+} brine) up to 90 °C (Figure 1c), which was consistent with the persistence of sufficient negative charge as shown in the electrophoretic mobility and the clear phase observed after 24 h. Moreover, the observed maintenance of D_H at high temperature was in good agreement with previous studies in which PSS and PAMPS copolymers in salt free solutions were shown to maintain their scattering profile in DI water up to 55 °C by small-angle X-ray and neutron scattering.[61,62] Additionally, macroscopically clear phases have been reported for poly(AMPS-*co*-acrylamide) copolymers in 3% $CaCl_2$ up to 100 °C.[25,26,63,64] Overall, the high acidity and hydrophilicity of the AMPS groups in poly(AMPS-*co*-AA) promoted hydration and reduced Ca^{2+}-affinity, providing excellent solvation even in the presence of PAA. The detailed characterization of poly(AMPS-*co*-AA) in highly concentrated API brine at 90 °C provided a basis for understanding its behavior as a stabilizer when grafted on NPs.

Properties and Stability of poly(AMPS-*co*-AA) Grafted IO NPs. To covalently attach the synthesized poly(AMPS-*co*-AA) copolymers to the surfaces of the IOs, we turned to the

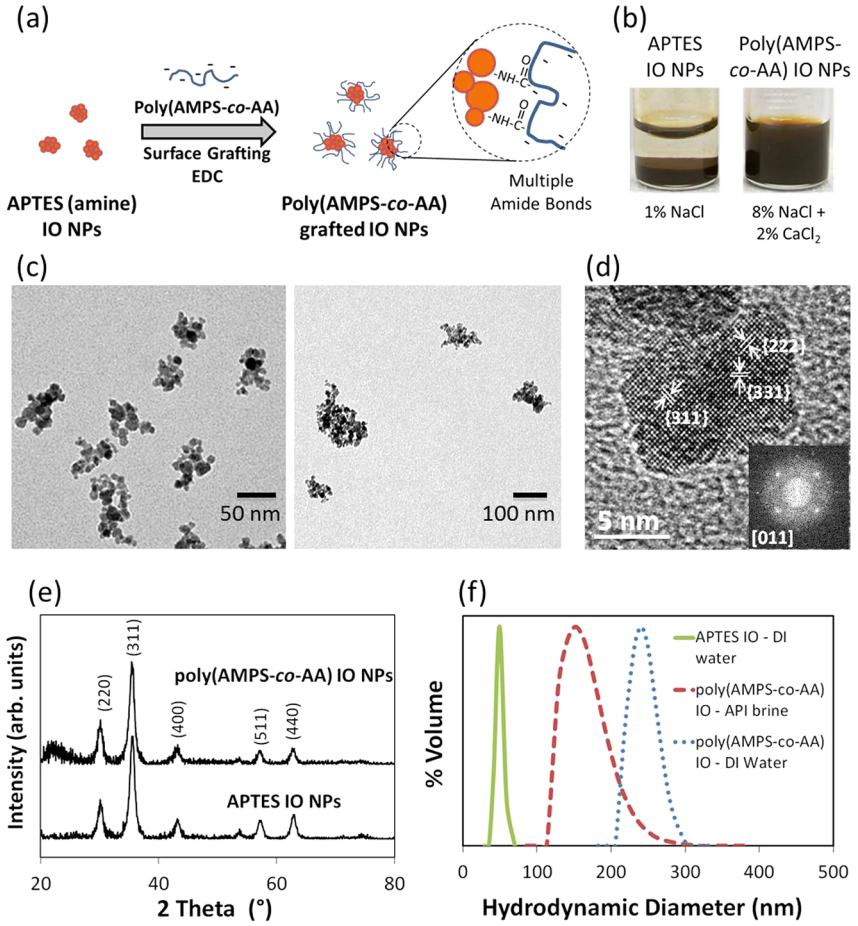

Figure 2. (a) Schematic of poly(AMPS-*co*-AA) multipoint grafting to APTES IO NPs via amidation. (b) Photographs of dispersions of APTES IO in 1% NaCl and poly(AMPS-*co*-AA) grafted IO NPs in API brine. (c) TEM images of APTES IO NPs (left) and poly(AMPS-*co*-AA) grafted IO NPs (right). (d) High-resolution TEM image of IO particle oriented with a [110] zone axis. (e) Powder XRD pattern of poly(AMPS-*co*-AA) grafted IO and APTES IO NPs. (f) Volume-weighted D_H distribution of APTES IO NPs in DI water, and poly(AMPS-*co*-AA) grafted IO NPs in DI water and API brine at pH 8.

"grafting-to" approach,[37,40,43,65] which generally enables direct attachment of preformed copolymers with desired molecular weight and well-defined composition. This approach circumvents the limitations associated with 'grafting-from' approaches,[17,39,66−68] including the need for surface-grafted initiators, exogenous catalysts and, in many cases, inert atmospheres.[19] Poly(AMPS-*co*-AA) was grafted to amine-functionalized IO NPs by condensing the carboxylate groups on the polymer with the IO surface amine groups, as catalyzed by 1-ethyl-3-(3-dimethylaminopropyl)carbodiimide (EDC) (Figure 2a). The surface amine groups were installed by conjugation of preformed IO NPs with (3-aminopropyl)-triethoxysilane (APTES) and confirmed by the following results: (i) a positive electrophoretic mobility of $+1.9 \times 10^{-8}$ $m^2/(V\ s)$ at pH 6 (Table 1), (ii) the presence of 7 wt % organics by thermogravimetric analysis (Table 1) and (iii) FTIR spectroscopy, which revealed the expected peaks corresponding to Si−O (1070 and 1150 cm^{-1}), N−H (1622, 1387, and 957 cm^{-1}) and C−H (2980 cm^{-1}) moieties (see Figure S5 in the Supporting Information). Analysis by transmission electron microscopy (TEM) revealed that ∼50 nm diameter nanoclusters (APTES IO) were composed of primary IO NPs with a mean diameter of 9.8 ± 2 nm (see Figure S6 in the Supporting Information). The high-resolution TEM indicates a ∼10 nm single-crystal particle, with few defects, and part of a particle above it within a nanocluster (Figure 2d). The *d*-spacing of {311}, {222}, and {331} planes as determined by Fourier analysis (Figure 2d inset), are 0.2478, 0.2493, and 0.1848 nm, respectively, which matched well with

Table 1. Summary of Colloidal and Magnetic Properties of IO Nanoclusters before and after Poly(AMPS-*co*-AA) Grafting

property	APTES IO NPs	poly(AMPS-*co*-AA) grafted IO NPs
hydrodynamic diameter D_H (nm)	55 ± 7[a,b]	165 ± 24[a,c]
electrophoretic mobility μ ($\times 10^{-8}$ $m^2/(V\ s)$)	+1.9 ± 0.3[a] (pH 6)	−2.8 ± 0.2[a] (pH 8)
% organics by TGA	7 ± 3[e]	15 ± 3[e]
magnetic susceptibility of IO liquid dispersion at 700 Hz (SI units)	0.105 (2.1 wt % IO)	0.083 (1.7 wt % IO)
magnetic susceptibility/g-Fe (SI units)[d]	7.0	6.8

[a]Reported value is the average of five independent experiments. [b]D_H of APTES IOs measured in DI water. [c]D_H of poly(AMPS-*co*-AA) grafted IOs measured in API brine. [d]Susceptibility of ∼2 wt % IO dispersion measured in DI water and converted to SI units (/g Fe). [e]TGA data were collected in an air atmosphere, 3% error is calculated by taking into account of possible oxidation of magnetite to maghemite/hematite at high temperature.

dx.doi.org/10.1021/am4003974 | ACS Appl. Mater. Interfaces 2013, 5, 3329−3339

the *d*-spacing of corresponding planes (0.2525, 0.2417, and 0.1921 nm, respectively) of bulk magnetite.[69] The five peaks in the powder XRD for both APTES and poly(AMPS-*co*-AA) grafted IO NPs (Figure 2e) also matched well with magnetite crystal phase (ICDD card No. 19−0629) with a crystallite size of 8 nm by Scherrer analysis that agrees with the mean primary particle diameter by TEM.[69] A D_H of 55 nm was measured for the APTES IO (Figure 2f and Table 1), which was in good agreement with the cluster diameter observed by TEM and was consistent with the small size of the aminopropyl groups on the surface (<1 nm).

The covalent grafting of the anionic poly(AMPS-*co*-AA) to the cationic amine surface at pH 6 was expected to be favorable by the electrostatic attraction at low graft densities; however further grafting should be inhibited as the graft density increases the negative charge in the brush layer. The grafting procedure was therefore performed in the presence of NaCl to screen the charges.[70] After grafting with anionic poly(AMPS-*co*-AA), the electrophoretic mobility was reversed to a negative value of -2.8×10^{-8} m^2/(V s) at pH 8 and the organic content increased to 15 ± 3 wt % as measured by TGA (Table 1). After grafting, the volume-based magnetic susceptibility of the liquid dispersion changed slightly from 7 to 6.8/(g Fe) (Table 1) and the saturation magnetization was also essentially unchanged at ∼90 emu/(g Fe) (Figure 3), indicating that the magnetic properties of IO NPs were not significantly affected by the grafting process. The high saturation magnetization, relative to the theoretical values of ∼120 emu/(g Fe) for bulk magnetite, was consistent with the high crystallinity of the NPs (Figure 2c, d). Moreover, the lower surface area of the clustered architecture compared to individual primary NPs leads to a low 15 ± 3 wt % organic loading on poly(AMPS-*co*-AA)-grafted IO NPs, which helps maintain a high magnetic mass loading. Further, the hysteresis curve of IO NPs demonstrates superparamagnetic-like behavior.

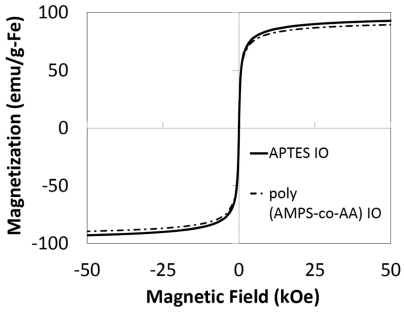

Figure 3. Room-temperature magnetization curves of APTES IO NPs before and after grafting with poly(AMPS-co-AA) (3:1) copolymer display very similar saturation magnetization at 92.9 and 89.5 emu/(g Fe), respectively.

The D_H of the IO particles in DI water increased from 55 ± 7 to 258 ± 34 nm, as determined by DLS and TEM (Figure 2f,c). The increase was much larger than expected from the grafting of poly(AMPS-*co*-AA) with a D_H of only 10 nm (Figure 1). Presumably, the grafting process led to aggregation of clusters, and/or to a process such as Ostwald ripening, whereby primary particles diffuse from smaller to larger clusters to lower the interfacial energy. Furthermore, the size of clusters may have been influenced by short-ranged attraction versus long-ranged repulsion between primary particles, which is generally mediated by the polymer.[71,72] Nonetheless, the poly(AMPS-*co*-AA) grafted IO NPs were found to form stable dispersions in API brine at room temperature, whereas before grafting, the APTES IO aggregated in only 1% NaCl (Figure 2b). Notably, the dispersions appeared uniform, visually stable and did not settle, thus demonstrating the first example of stabilization of polyelectrolyte coated inorganic NPs at high divalent salinity. Moreover, the dispersions maintained their stability at elevated temperature (90 °C), a feat which has only rarely been reported for metal oxide particles.[16,73] The stability of the dispersions suggested that the polymer chains remained solvated in the brine and provided excellent steric stabilization. The exceptional stability was corroborated by measuring the D_H in API brine at room temperature and at 90 °C over an extended period of time (Figure 4). Notably, a decrease in D_H from 258 ± 34 nm in DI water to 165 ± 24 nm in API brine (Table 1 and Figure 2f) was observed, which may have been caused by an increased cluster density due to weaker electrostatic repulsion between primary particles[18] and/or reduced osmotic swelling.[56,59] Regardless, the D_H measured in API brine at 90 °C remained constant (D_H = 180−200 nm) over a period of 30 days, demonstrating that the clusters were exceptionally stable, and that only a negligible amount of aggregation occurred

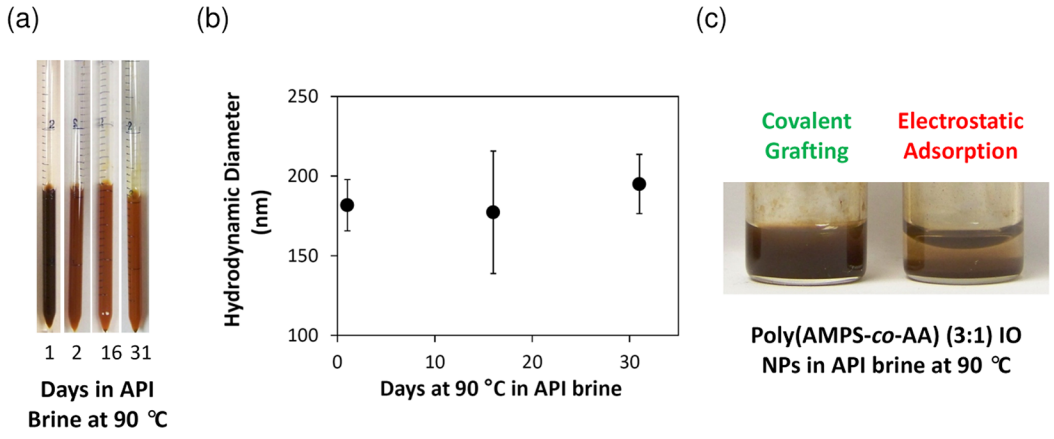

Figure 4. poly(AMPS-*co*-AA) grafted APTES IOs were stable in API brine at 90 °C for 31 days, as evidenced by (a) visual inspection and (b) constant hydrodynamic diameters D_H in API brine. (c) After a 40 000-fold serial dilution in 1 M NaCl, poly(AMPS-*co*-AA) grafted APTES IO NPs remained stable at 0.2 wt % IO in API brine at 90 °C (left), whereas IO NPs with electrostatically attached poly(AMPS-*co*-AA) aggregated.

(Figure 4b). Together with the visual observations (Figure 4a), the high-temperature DLS results confirmed that the grafted IO NPs exhibited remarkable colloidal stability in API brine at 90 °C for 1 month. To the best of our knowledge, this result is the first demonstration of long-term stability of inorganic NPs at elevated temperature and high divalent salinity.

Subsequent efforts were directed toward determining whether the poly(AMPS-*co*-AA) chains were covalently grafted to the IO NP surface, rather than physically adsorbed. To this end, the dispersions were diluted by a factor of 40,000 to concentrations of 0.01% w/v IO. After dilution, the recovered particles were found to be stable in API brine at 90 °C for at least 24 h at a concentration of 0.2% w/v IO indicating that the polymer remained on the IO NP surface. In contrast, when no EDC was used during the grafting process and poly(AMPS-*co*-AA) was simply electrostatically adsorbed onto IO NPs, the particles aggregated in less than 30 min in API brine at 90 °C after the dilution was conducted (Figure 4c). Presumably after such a drastic dilution the highly hydrophilic polymer would desorb from the NP surface and diffuse into the aqueous phase if not covalently attached, thus the observed stability of the particles treated with polymer and EDC strongly suggests that the polymer is covalently attached to the IO. Moreover, for the grafted case, TGA indicated 15% organic material (polymer and citrate ligands) before the dilution test. Given that this is a relatively small amount, most of the polymer was likely grafted. Unfortunately, attempts to investigate the grafting via IR spectroscopy to identify amide bonds between poly(AMPS-*co*-AA) and amine IOs were ineffective given the inability to distinguish between the signals corresponding to the grafted amides from those in the AMPS side groups. As an alternative control, PAA homopolymer was grafted to APTES IOs via the aforementioned EDC-catalyzed amidation method. A broad signal at 1700 cm^{-1} (see Figure S5 in the Supporting Information) was observed and indicated that amide bonds were formed between PAA and APTES IO. On the contrary, when EDC was not used, no amide signal was observable in the IR spectrum.

As demonstrated by the dilution test, the covalent bonding of poly(AMPS-*co*-AA) to the NP surfaces provided much more robust attachment than chemisorption, for example by reversible charge-transfer complexes between iron cations and polycarboxylates as shown in Figures 2 and 3.[6,16,18,28,34,56,65] Furthermore, unlike the generally reported single covalent bond attachment of terminal functional polymer chains,[56,65] a key advancement of our approach is the attachment of poly(AMPS-*co*-AA) chains through the formation of multiple bonds.[41,42] The stable amide bonds between IO NPs and poly(AMPS-*co*-AA) ensured that the AMPS groups maintained steric stabilization. Even if a fraction of the covalent bonds degraded, multiple attachments were still left, which may have helped maintain colloidal stability of poly(AMPS-*co*-AA) grafted IO NPs in API brine at 90 °C even after a 40 000-fold dilution (Figure 4c).

The electrophoretic mobilities (μ) of poly(AMPS-*co*-AA) grafted IO NPs were measured in a series of NaCl and $CaCl_2$ solutions (Figure 5) with a fixed molar ratio of 7.6:1, which is analogous to the ratio in API brine. At low salinity, the μ was observed to be highly negative, -3×10^{-8} $m^2/(V\ s)$ in DI water (0.03 mM), reflecting the large number of charges in the polyelectrolyte. The magnitude of the mobility decreased to -2×10^{-8} $m^2/(V\ s)$ in a 10 mM solution of combined Na^+ and Ca^{2+} (at 7.6: 1 mol ratio), and remained constant within

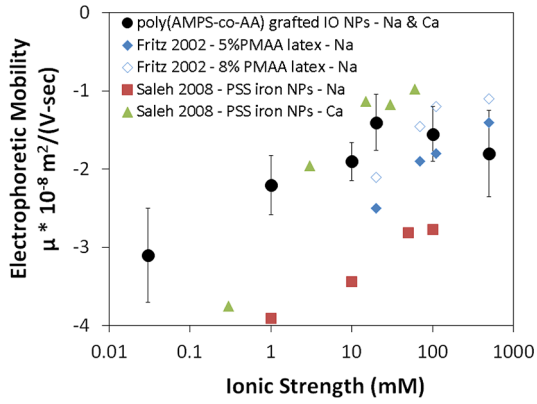

Figure 5. Plot of electrophoretic mobility of poly(AMPS-*co*-AA) grafted IO NPs versus ionic strength in combined Na^+ and Ca^{2+} solutions (Na^+:Ca^{2+} mole ratio = 7.6, same as API brine) at pH 8 (black circles) compared with literature mobility data for other polyelectrolyte-coated NPs including PMAA-stabilized latex (Fritz 2002)[17] (blue diamonds) and PSS-coated iron NPs (Saleh 2008)[6] (green triangles, red squares).

experimental error at a value of -1.8×10^{-8} $m^2/(V\ s)$ in 500 mM NaCl and $CaCl_2$. Unlike the measurements described above (Figure 1d) with pure poly(AMPS-*co*-AA), μ of the grafted NPs could not be measured above 500 mM due to a large growth in experimental uncertainty, which is quite common for extreme salinities.[6,17] The reduction in magnitude to a μ of -1.8×10^{-8} $m^2/(V\ s)$ at 0.5 M ionic strength (380 mM Na^+ and 50 mM Ca^{2+}) suggested that significant screening of the charges on the polyelectrolyte occurred, as expected at such high ionic strength. However, the residual mobility indicated that the Ca^{2+} did not bind all of the sulfonate groups, as was also observed for the pure poly(AMPS-*co*-AA) (Figure 1d).

The remarkable stability of the poly(AMPS-*co*-AA) grafted IO NPs may be explained by established concepts in colloid chemistry. According to Napper,[20] the colloidal stability of the poly(AMPS-*co*-AA) grafted IO NPs (Figure 4) at all salinities and temperatures may be anticipated given the limited collapse of the pure polymer (Figure 1b). The total interaction potential between two polymer coated particles is a function of steric repulsion, electrostatic repulsion and van der Waals attraction. At high salinity (e.g., API brine), electrostatic interactions within the polyelectrolyte layer are screened by the ions and the brush may be considered as a neutral polymer.[17,68] The steric repulsion to the energy barrier comes from two distinct mechanisms: (i) osmotic repulsion between overlapping chains and (ii) entropy of elastic repulsion.[17,28] The osmotic repulsion depends upon the particle diameter, the brush length relative to the distance between particle surfaces, the polymer volume fraction in the brush layer, and the Flory–Huggins interaction parameter χ.

The equilibrium structure of dense polyelectrolyte brushes is governed by a balance between short-ranged excluded volume, long-range electrostatic interactions and the osmotic effects of the counterions in the brush layer, in many ways as described above for pure polyelectrolytes. At low salt concentrations, highly concentrated confined counterions in the brush generate an osmotic pressure that stretches the chains. However, when the concentration of added salt approaches the ion concentration within the brush layer, screening of the electrostatic repulsion and reduction in the osmotic pressure cause the

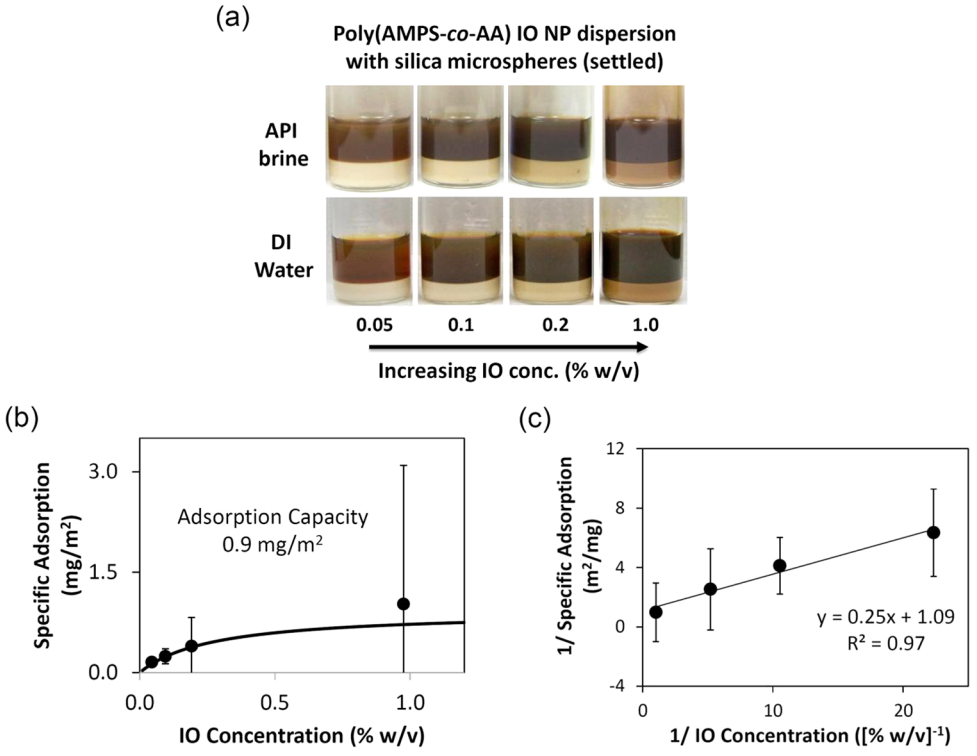

Figure 6. (a) Photographs of poly(AMPS-*co*-AA)-grafted iron oxide (IO) nanoclusters in API brine (top) and DI water (bottom) displaying very low adsorption on silica at IO concentrations ranging from 0.05 to 1% w/v IO. Each sample vial contains 2 mL of IO dispersion at pH 8 and 1 g of colloidal silica and was equilibrated for 16−20 h. IO adsorption isotherm data in API brine expressed (b) as fit to a Langmuir adsorption model in standard units and (c) inverse units.

brushes to contract.[59] Eventually, the highly screened polyelectrolyte brush will behave similarly to an uncharged brush.[59,67] The contraction of polymer brushes with increased salinity was observed by DLS for polymethacrylic acid (PMAA) coated latex NPs, where the brush thickness decreased from 22.3 nm at 100 mM NaCl to 15.8 nm at only 500 mM NaCl at pH 7.[17] Similarly, the thickness of PSS brushes on latex NPs decreased from 65 nm at 0.1 mM Mg^{2+} to 28 nm at 100 mM Mg^{2+}.[67]

The charge density of the brush layer, which influences the brush conformation, may be studied directly in terms of the electrophoretic mobility. Relatively few studies have reported μ of anionic polyelectrolyte-coated NPs up to the high salinity levels shown in Figure 5.[6,17,28] In general, for each of these colloids coated with various anionic polyelectrolytes, the magnitude of the mobility decreased with ionic strength, but was still more than -1×10^{-8} $m^2/(V\ s)$, even at an ionic strength of 0.5 M. The overall decrease in magnitude was less than 2-fold in nearly all cases. An exception was PSS-coated iron NPs, for which the change was much larger in Ca^{2+} than Na^+ solutions,[6] which was consistent with the stronger electrostatic attraction for Ca^{2+} and specific binding observed by NMR spectroscopy.[27,50] The mobility of the more hydrophilic poly(AMPS-*co*-AA) grafted IO NPs remained more negative and measurable at a higher ionic strength of 500 mM relative to only 60 mM for the more hydrophobic PSS. Interestingly, the μ for poly(AMPS-*co*-AA) IO NPs was negative at 0.5 M for the combined Ca^{2+} and Na^+ electrolyte as well as for Na^+ independently in the case of PMAA latex NPs, despite the stronger electrostatic interactions with the divalent cation. Thus, the high fraction of AMPS functional groups, which do not bind Ca^{2+} specifically, were effective for maintaining a significant poly(AMPS-*co*-AA) mobility and thus particle charge even at extremely high salinity. Given the observed particle mobility in addition to the morphology of the pure polymer measured by DLS, it is likely that the grafted chains on the IO nanoclusters are only partially collapsed, which is further consistent with the impressive colloidal stability.

Steric stabilization has been demonstrated in solutions of up to 5 M NaCl at room temperature for NPs coated with PAA,[31] PMAA[17] and copolymers containing PVS and/or PSS.[6,16] Here, the segment-solvent interactions were favorably attractive ($\chi < 1/2$) because of the weak affinity of Na^+ for the carboxylate or sulfonate anions. When divalent ions were present, however, the PSS-coated iron NPs were stable only up to 100 mM Ca^{2+} at room temperature,[6] and PSS-grafted latex NPs precipitated above 100 mM Mg^{2+}.[67] These results were consistent with partial chain collapse of PSS in the presence of divalent ions as observed by SANS[51] and NMR.[60] The divalent ion binding is likely promoted by dehydration of the sulfonate groups because of the hydrophobicity of the styrene group. Thus, the PSS segment-solvent interactions became repulsive ($\chi > 1/2$) at high divalent ion concentrations causing loss of steric stabilization.[74] In contrast, poly(AMPS-*co*-AA) grafted IO NPs remained stable in highly concentrated API brine at both room temperature and at 90 °C. The highly hydrophilic and acidic AMPS groups that bind weakly to Ca^{2+} ensured attractive PAMPS segment-solvent interactions even in the presence of Ca^{2+} with a favorable χ (<1/2) for steric stabilization in API brine. The favorable χ is also evident in the phase behavior and conformation of the pure polymer. When the distance of approach between two NPs becomes closer than the brush thickness, compression of the polymer

chains causes a loss in entropy or elastic repulsion. The high MW of poly(AMPS-*co*-AA) and graft density each contribute to the high entropic elastic repulsion contribution.[70] Finally, the residual charge, as shown in the electrophoretic mobility, provides a degree of electrostatic repulsion between overlapping brushes that further contributes to the colloidal stability. In summary, the highly screened polymer brushes behaved as neutral brushes with favorable solvation to provide steric stabilization even at high temperatures in API brine, similarly to the earlier results for PMAA in NaCl brines at room temperature.[17]

Adsorption of Poly(AMPS-*co*-AA)-Grafted IO NPs on Silica. The batch adsorption technique allowed for rapid, high throughput measurement of equilibrium NP adsorption behavior relative to the measurement of NP retention in flow experiment in porous media,[7] where additional effects of filtration[6,75,76] and hydrodynamics may be present.[8,77,78] The IO adsorption on silica microspheres was visually observed and quantified by measuring the change in IO concentration before and after equilibration (Figure 6 and Table 2.) Experiments were conducted in either DI water or API brine, and after overnight equilibration at pH 8, the settled silica microspheres were white in 0.05−0.1% w/v IO and lightly brown colored in 1.0% w/v IO. When measured in DI water, the difference between the initial and final concentration, reported as % IO adsorbed, was small (≤2%). On the basis of the volume of the solution and the surface area of silica, the calculated specific adsorption values were smaller than the experimental uncertainty and hence only upper bounds are reported. At the highest IO concentration (1% w/v) in DI water, the specific adsorption was <1.1 mg-IO/m^2 silica. In API brine, the % IO adsorbed was modestly higher than in DI water. The calculated specific adsorption in API brine at the highest IO concentration of (1% w/v) was 1.0 ± 2.1 mg/m^2 which corresponds to a very low NP monolayer coverage of 0.4%. In contrast, when polymer was only adsorbed electrostatically, the IO NP sample resulted in 48% adsorption in API brine at 0.103% w/v IO equilibrium concentration to give a specific adsorption value of 16.6 mg/m^2 or 8.6% monolayer coverage.

Table 2. Adsorption of Poly(AMPS-*co*-AA) IO Nanoclusters on 8 μm Colloidal Silica Microspheres in API Brine and DI Water at pH 8 at Varying IO Concentrations.[a]

initial IO conc. (% w/v)	medium	% IO adsorbed[b]	final eq. IO conc (% w/v)[b]	specific adsorption (mg IO/m^2)[b]	% monolayer
0.1	DI water	2	0.098	<0.04	<0.03
0.2	DI water	2	0.197	<0.11	<0.05
1.0	DI water	1	1.00	<1.1	<0.4
0.05	API brine	7	0.047	0.16 ± 0.07	0.1
0.1	API brine	5	0.095	0.24 ± 0.11	0.1
0.2	API brine	4	0.192	0.4 ± 0.4	0.2
1.0	API brine	2	0.975	1.0 ± 2.1	0.4
0.2[c]	API brine	48[c]	0.103[c]	16.6 ± 1.3[c]	8.6[c]

[a]The specific surface area of colloidal silica was measured to be ∼0.58 m^2/g. [b]Average of four independent experiments; uncertainty in specific adsorption based on error propagation analysis. [c]Control sample data at 0.2% w/v initial IO conc. is also shown as an example of IOs with high adsorption where insufficient polymer grafting leads to poor stabilization. Adsorption was conducted with 0.2 g of silica and 2 mL of IO NP dispersion.

The adsorption isotherm displayed in Figure 6 exhibited Langmuir behavior. A linearized Langmuir plot of IO adsorption in inverse IO concentration and specific adsorption units (Figure 6c) resulted in a reasonable correlation coefficient (R^2 = 0.97) where the slope (0.25 × 10^7 m^{-1}) and intercept (1.09 m^2/mg-IO) are expressed as shown in eqs 1 and 2 below.

$$m = \left(\frac{k_{des}}{k_{ads}}\right)\left(\frac{\rho_a}{A_c}\right)M_p \quad (1)$$

$$b = \frac{\rho_a}{A_c} \quad (2)$$

In the above equations, k_{des}/k_{ads} is the ratio of the rate of desorption to the rate of adsorption (m^{-3}), M_p is the mass of one NP (g), A_c is the adsorption capacity on the collector surface (g IO/g silica), and ρ_a is the specific surface area of silica (m^2/(g silica)). Using the specific surface area of the silica, A_c can be converted to ((mg IO)/(m^2 silica)). The specific adsorption capacity A_c was 0.9 (mg IO)/(m^2 silica) (or 0.4% monolayer) and the equilibrium constant (k_{des}/k_{ads}) 3.2 × 10^{17} m^3 (Figure 6c). To the best of our knowledge, this is the first report demonstrating low equilibrium adsorption capacity of iron oxide NPs on silica in high salinity (1.8 M ionic strength) and with high divalent ion concentration (180 mM Ca^{2+}).

The low adsorption for poly(AMPS-*co*-AA) grafted IO NPs suggested to us that the well-solvated extended polymer chains on the surface provided steric stabilization with the silica surface. The chain extension again reflects high acidity and high hydrophilicity for the polymer with low Ca^{2+} affinity. Here only the particle surface contained polymer chains for steric repulsion, unlike the case of the interactions between two polymer-coated NPs.[8] However, a single steric polymer layer in conjunction with the electrostatic repulsion with the anionic silica surface provided sufficient repulsion to produce very low adsorption. Notably, the observed adsorption of the poly(AMPS-*co*-AA)-coated IO NPs was significantly lower at higher IO concentrations and higher ionic strength than previously reported polymer-coated zerovalent iron (ZVI) NPs on quartz sand or silica sand.[6]

CONCLUSIONS

IO NPs with permanently grafted poly(AMPS-*co*-AA) copolymers exhibited long-term (≤1 month) steric stabilization at high salinities and elevated temperatures (up to 90 °C). A high ratio of the stabilizer group, AMPS, to the AA anchor group (3:1 AMPS:AA) in the polymer coating maintained sufficient chain solubility even at extreme salinities of 8 wt % NaCl + 2 wt % $CaCl_2$ (API brine). Furthermore, the AA anchor groups enabled multipoint covalent grafting for robust attachment of the polymer coating to the IO surface, which prevented polymer desorption even after a 40 000 fold dilution. The poly(AMPS-*co*-AA) polymer itself was also found to be resistant to chain collapse in the presence of Na^+ and Ca^{2+} at both 25 and 90 °C, as evidenced by DLS and electrophoretic mobility measurements, which was consistent with previous reports using the analogous homopolymers.[27] Therefore, when grafted on the IO NPs, the extended highly solvated polymer

chains resulted in remarkable steric stabilization of the NPs and extremely low adsorption on silica surfaces even at the extreme API brine salinity. Moreover, the IO NPs retained their magnetic susceptibilities after both amine functionalization and polymer the grafting. To the best of our knowledge, this is the first example of colloidal stability and low mineral adsorption of metal oxide NPs at such high ionic strength and elevated temperatures. NPs with such remarkable behavior at extreme salinities and temperatures are expected to find utility in a vast array of applications, including transport through subsurface porous media for enhanced oil recovery, environmental remediation, CO_2 sequestration, and to facilitate electromagnetic imaging of hydrocarbon reservoirs.

■ ASSOCIATED CONTENT

Supporting Information

Images of silica microspheres; ^1H and ^{13}C NMR spectra of poly(AMPS-*co*-AA); correlation of hydrodynamic diameter of polymer and degree of polymerization; hydrodynamic diameter of poly(AMPS-*co*-AA) in various Ca^{2+} media; IR spectra of PAA grafted IO NPs; magnetization curves of IO NPs before and after poly(AMPS-*co*-AA) grafting. This material is available free of charge via the Internet at http://pubs.acs.org.

■ AUTHOR INFORMATION

Corresponding Author

*E-mail: kpj@che.utexas.edu.

Author Contributions

‡Authors H.G.B and Z.X. contributed equally.

Notes

The authors declare no competing financial interest.

■ ACKNOWLEDGMENTS

This work was supported by the Advanced Energy Consortium. Member companies include Shell, Halliburton Energy Services Inc., Petrobras, Schlumberger, BP America Inc., ConocoPhillips, Total and BG Group and the NSF (CBET-0968038). C.W.B. and K.P.J. are grateful to the Welch Foundation (F-1621 and F-1319, respectively) for support. K.P.J. is also grateful for funds from Gulf of Mexico Research Initiative. We thank Mr. William Hardin for assistance with XRD and HR-TEM analysis, and Mr. Daniel Groom for collection of HR-TEM images.

■ REFERENCES

(1) Halford, B. *Chem. Eng. News* **2012**, *90*, 60.
(2) Kanj, M. Y.; Rashid, M. H.; Giannelis, E. In *SPE Middle East Oil and Gas Show and Conference*; Manama, Bahrain, 2011 ; Society of Petroleum Engineers: Richardson, TX, 2011.
(3) Jikich, S. A.; , *J. Pet. Technol.* **2012**, *July*, 28.
(4) Javadpour, F.; Nicot, J. P. *Transp. Porous Media* **2011**, *89*, 265.
(5) Worthen, A. J.; Bagaria, H. G.; Chen, Y.; Bryant, S. L.; Huh, C.; Johnston, K. P. *J. Colloid Interface Sci.* **2013**, *398*, 217.
(6) Saleh, N.; Kim, H. J.; Phenrat, T.; Matyjaszewski, K.; Tilton, R. D.; Lowry, G. V. *Environ. Sci. Technol.* **2008**, *42*, 3349.
(7) Wang, Y. G.; Li, Y. S.; Fortner, J. D.; Hughes, J. B.; Abriola, L. M.; Pennell, K. D. *Environ. Sci. Technol.* **2008**, *42*, 3588.
(8) Petosa, A. R.; Jaisi, D. P.; Quevedo, I. R.; Elimelech, M.; Tufenkji, N. *Environ. Sci. Technol.* **2010**, *44*, 6532.
(9) Laurent, S.; Forge, D.; Port, M.; Roch, A.; Robic, C.; Elst, L. V.; Muller, R. N. *Chem. Rev.* **2008**, *108*, 2064.
(10) Jeong, U.; Teng, X. W.; Wang, Y.; Yang, H.; Xia, Y. N. *Adv. Mater.* **2007**, *19*, 33.
(11) Kotsmar, C.; Yoon, K. Y.; Yu, H. Y.; Ryoo, S. Y.; Barth, J.; Shao, S.; Prodanovic, M.; Milner, T. E.; Bryant, S. L.; Huh, C.; Johnston, K. P. *Ind. Eng. Chem. Res.* **2010**, *49*, 12435.
(12) Ryoo, S.; Rahmani, A. R.; Yoon, K. Y.; Prodanovic, M.; Kotsmar, C.; Milner, T. E.; Johnston, K. P.; Bryant, S. L.; Huh, C. *J. Pet. Sci. Eng.* **2012**, *81*, 129.
(13) Sanni, M. L.; Yeh, N.; N. I. Al-Afaleg, A. U. Al-Kaabi, Levesque, C.; Donadille, J.-M.; Ma, S. M. In *SPE Middle East Oil and Gas Show and Conference*; Manama, Bahrain, 2007 ; Society of Petroleum Engineers: Richardson, TX, 2007.
(14) Liang, L.; Abubakar, A.; Habashy, T. In *SPE Annual Technical Conference and Exhibition*; Florence, Italy, 2010 Society of Petroleum Engineers: Richardson, TX, 2010.
(15) Berlin, J. M.; Yu, J.; Lu, W.; Walsh, E. E.; Zhang, L. L.; Zhang, P.; Chen, W.; Kan, A. T.; Wong, M. S.; Tomson, M. B.; Tour, J. M. *Energy Environ. Sci.* **2011**, *4*, 505.
(16) Ditsch, A.; Laibinis, P. E.; Wang, D. I. C.; Hatton, T. A. *Langmuir* **2005**, *21*, 6006.
(17) Fritz, G.; Schadler, V.; Willenbacher, N.; Wagner, N. J. *Langmuir* **2002**, *18*, 6381.
(18) Yoon, K. Y.; Kotsmar, C.; Ingram, D. R.; Huh, C.; Bryant, S. L.; Milner, T. E.; Johnston, K. P. *Langmuir* **2011**, *27*, 10962.
(19) Zhang, L.; Xue, H.; Gao, C. L.; Carr, L.; Wang, J. N.; Chu, B. C.; Jiang, S. Y. *Biomaterials* **2010**, *31*, 6582.
(20) Napper, D. H. *Polymeric Stabilization of Colloidal Dispersions*; Academic Press: New York, 1983.
(21) Hiemenz, P. C.; Rajagopalan, R. *Principles of Colloid and Surface Chemistry*; Marcel Dekker: New York, 1997.
(22) Buscall, R.; Corner, T. *Eur. Polym. J.* **1982**, *18*, 967.
(23) Schweins, R.; Huber, K. *Eur. Phys. J. E* **2001**, *5*, 117.
(24) Lages, S.; Lindner, P.; Sinha, P.; Kiriy, A.; Stamm, M.; Huber, K. *Macromolecules* **2009**, *42*, 4288.
(25) Mccormick, C. L.; Elliott, D. L. *Macromolecules* **1986**, *19*, 542.
(26) Hsieh, H. L.; Moradiaraghi, A.; Stahl, G. A.; Westerman, I. J. *Makromol. Chem., Macromol. Symp.* **1992**, *64*, 121.
(27) Newman, J. K.; Mccormick, C. L. *Macromolecules* **1994**, *27*, 5114.
(28) Phenrat, T.; Saleh, N.; Sirk, K.; Kim, H. J.; Tilton, R. D.; Lowry, G. V. *J. Nanopart. Res.* **2008**, *10*, 795.
(29) Guo, X.; Weiss, A.; Ballauff, M. *Macromolecules* **1999**, *32*, 6043.
(30) Chen, K. L.; Mylon, S. E.; Elimelech, M. *Environ. Sci. Technol.* **2006**, *40*, 1516.
(31) Guo, X.; Ballauff, M. *Phys. Rev. E* **2001**, 64.
(32) Wagener, P.; Schwenke, A.; Barcikowski, S. *Langmuir* **2012**, *28*, 6132.
(33) Park, J. J.; Lacerda, S. H. D. P.; Stanley, S. K.; Vogel, B. M.; Kim, S.; Douglas, J. F.; Raghavan, D.; Karim, A. *Langmuir* **2009**, *25*, 443.
(34) Ge, J. P.; Hu, Y. X.; Biasini, M.; Dong, C. L.; Guo, J. H.; Beyermann, W. P.; Yin, Y. D. *Chem.—Eur. J.* **2007**, *13*, 7153.
(35) Ersenkal, D. A.; Ziylan, A.; Ince, N. H.; Acar, H. Y.; Demirer, M.; Copty, N. K. *J. Contam. Hydrol.* **2011**, *126*, 248.
(36) Chanteau, B.; Fresnais, J.; Berret, J. F. *Langmuir* **2009**, *25*, 9064.
(37) Barrera, C.; Herrera, A. P.; Bezares, N.; Fachini, E.; Olayo-Valles, R.; Hinestroza, J. P.; Rinaldi, C. *J. Colloid Interface Sci.* **2012**, *377*, 40.
(38) Amstad, E.; Textor, M.; Reimhult, E. *Nanoscale* **2011**, *3*, 2819.
(39) Lattuada, M.; Hatton, T. A. *Langmuir* **2007**, *23*, 2158.
(40) Boyer, C.; Whittaker, M. R.; Bulmus, V.; Liu, J. Q.; Davis, T. P. *NPG Asia Mater.* **2010**, *2*, 23.
(41) Peng, J. X.; Liu, Q. X.; Xu, Z. H.; Masliyah, J. *Adv. Funct. Mater.* **2012**, *22*, 1732.
(42) Ujiie, K.; Kanayama, N.; Asai, K.; Kishimoto, M.; Ohara, Y.; Akashi, Y.; Yamada, K.; Hashimoto, S.; Oda, T.; Ohkohchi, N.; Yanagihara, H.; Kita, E.; Yamaguchi, M.; Fujii, H.; Nagasaki, Y. *Colloids Surf., B* **2011**, *88*, 771.
(43) Lopez-Cruz, A.; Barrera, C.; Calero-DdelC, V. L.; Rinaldi, C. *J. Mater. Chem.* **2009**, *19*, 6870.
(44) Massart, R. *IEEE Trans. Magn.* **1981**, *17*, 1247.

(45) Bee, A.; Massart, R.; Neveu, S. *J. Magn. Magn. Mater.* **1995**, *149*, 6.
(46) Feng, B.; Hong, R. Y.; Wang, L. S.; Guo, L.; Li, H. Z.; Ding, J.; Zheng, Y.; Wei, D. G. *Colloids Surf., A* **2008**, *328*, 52.
(47) Salon, M. C. B.; Belgacem, M. N. *Colloids Surf., A* **2010**, *366*, 147.
(48) Paquet, O.; Salon, M. C. B.; Zeno, E.; Belgacem, M. N. *Mater. Sci. Eng., C* **2012**, *32*, 487.
(49) Bernard, O.; Turq, P.; Blum, L. *J. Phys. Chem.* **1991**, *95*, 9508.
(50) Bohme, U.; Scheler, U. *Adv. Colloid Interface Sci.* **2010**, *158*, 63.
(51) Dubois, E.; Boue, F. *Macromolecules* **2001**, *34*, 3684.
(52) Combet, J.; Isel, F.; Rawiso, M.; Boue, F. *Macromolecules* **2005**, *38*, 7456.
(53) Sadeghpour, A.; Vaccaro, A.; Rentsch, S.; Borkovec, M. *Polymer* **2009**, *50*, 3950.
(54) Turesson, M.; Labbez, C.; Nonat, A. *Langmuir* **2011**, *27*, 13572.
(55) Sinn, C. G.; Dimova, R.; Antonietti, M. *Macromolecules* **2004**, *37*, 3444.
(56) Ballauff, M.; Borisov, O. *Curr. Opin. Colloid Interface Sci.* **2006**, *11*, 316.
(57) Dobrynin, A. V.; Rubinstein, M. *Prog. Polym. Sci.* **2005**, *30*, 1049.
(58) Rubinstein, M.; Papoian, G. A. *Soft Matter* **2012**, *8*, 9265.
(59) Israels, R.; Leermakers, F. A. M.; Fleer, G. J.; Zhulina, E. B. *Macromolecules* **1994**, *27*, 3249.
(60) Bohme, U.; Hanel, B.; Scheler, U. *Prog. Colloid Pol. Sci. S* **2011**, *138*, 45.
(61) Boue, F.; Cotton, J. P.; Lapp, A.; Jannink, G. *J. Chem. Phys.* **1994**, *101*, 2562.
(62) Essafi, W.; Haboubi, N.; Williams, C.; Boue, F. *J. Phys. Chem. B* **2011**, *115*, 8951.
(63) Rashidi, M.; Blokhus, A. M.; Skauge, A. *J. Appl. Polym. Sci.* **2011**, *119*, 3623.
(64) Levitt, D. B.; Slaughter, W.; Pope, G. A.; Jouenne, S. *SPE Reservior Eval. Eng.* **2011**, *14*, 287.
(65) Zdyrko, B.; Luzinov, I. *Macromol. Rapid Commun.* **2011**, *32*, 859.
(66) Saleh, N.; Sarbu, T.; Sirk, K.; Lowry, G. V.; Matyjaszewski, K.; Tilton, R. D. *Langmuir* **2005**, *21*, 9873.
(67) Mei, Y.; Ballauff, M. *Eur. Phys. J. E* **2005**, *16*, 341.
(68) Lozsan, A. E.; Romero-Cano, M. S. *J. Colloid Interface Sci.* **2011**, *354*, 70.
(69) Yathindranath, V.; Rebbouh, L.; Moore, D. F.; Miller, D. W.; van Lierop, J.; Hegmann, T. *Adv. Funct. Mater.* **2011**, *21*, 1457.
(70) Seyrek, E.; Hierrezuelo, J.; Sadeghpour, A.; Szilagyi, I.; Borkovec, M. *Phys. Chem. Chem. Phys.* **2011**, *13*, 12716.
(71) Johnston, K. P.; Maynard, J. A.; Truskett, T. M.; Borwankar, A. U.; Miller, M. A.; Wilson, B. K.; Dinin, A. K.; Khan, T. A.; Kaczorowski, K. J. *ACS Nano* **2012**, *6*, 1357.
(72) Tam, J. M.; Murthy, A. K.; Ingram, D. R.; Nguyen, R.; Sokolov, K. V.; Johnston, K. P. *Langmuir* **2010**, *26*, 8988.
(73) Jain, N.; Wang, Y.; Jones, S. K.; Hawkett, B. S.; Warr, G. G. *Langmuir* **2010**, *26*, 4465.
(74) Radeva, T., *Physical Chemistry of Polyelectrolytes*; Marcel Dekker: New York, 2001.
(75) Jaisi, D. P.; Saleh, N. B.; Blake, R. E.; Elimelech, M. *Environ. Sci. Technol.* **2008**, *42*, 8317−8323.
(76) Saleh, N.; Sirk, K.; Liu, Y. Q.; Phenrat, T.; Dufour, B.; Matyjaszewski, K.; Tilton, R. D.; Lowry, G. V. *Environ. Eng. Sci.* **2007**, *24*, 45.
(77) Zhang, M.; Akbulut, M. *Langmuir* **2011**, *27*, 12550.
(78) Mays, D. C.; Hunt, J. R. *Environ. Sci. Technol.* **2005**, *39*, 577.